

AUTHOR QUERY FORM

	<p>Journal: TUST</p> <p>Article Number: 1319</p>	<p>Please e-mail or fax your responses and any corrections to:</p> <p>E-mail: corrections.esch@elsevier.sps.co.in</p> <p>Fax: +31 2048 52799</p>
---	--	--

Dear Author,

Please check your proof carefully and mark all corrections at the appropriate place in the proof (e.g., by using on-screen annotation in the PDF file) or compile them in a separate list. To ensure fast publication of your paper please return your corrections within 48 hours.

For correction or revision of any artwork, please consult <http://www.elsevier.com/artworkinstructions>.

Any queries or remarks that have arisen during the processing of your manuscript are listed below and highlighted by flags in the proof. Click on the 'Q' link to go to the location in the proof.

Location in article	Query / Remark: click on the Q link to go Please insert your reply or correction at the corresponding line in the proof
<p>Q1</p> <p>Q2</p>	<p>Please check whether the identification of corresponding author is okay as typeset.</p> <p>Please note that the reference 'Molins and Arnau (2010)' cited in text but not in list. Kindly check.</p>

Thank you for your assistance.

Highlights

► 2D-plane stress and 3D-shell simulation of the L9 tunnel test performed in Barcelona. ► Detailed modeling of joints, ground-structure interaction and SFRC response. ► Excellent accuracy achieved in terms of displacements and joints closures. ► Validation of the SFRC adopted model by comparing the obtained crack patterns.

DF



Contents lists available at ScienceDirect

Tunnelling and Underground Space Technology

journal homepage: www.elsevier.com/locate/tust



Experimental and analytical study of the structural response of segmental tunnel linings based on an *in situ* loading test. Part 2: Numerical simulation

Oriol Arnau*, Climent Molins

Department of Construction Engineering, Universitat Politècnica de Catalunya (UPC), Jordi Girona 1-3, C1, 08034 Barcelona, Spain

ARTICLE INFO

Article history:
Available online xxx

Keywords:
Segmental tunnel linings
Structural analysis
Numerical simulation
SFRC
Ground-structure interaction
Joints behavior

ABSTRACT

The numerical simulation of the *in situ* test described in the part 1 of the paper is performed by means of two different approaches: a 2D plane stress model and a 3D shell elements model. A consistent modeling of the tunnel behavior is achieved through the proper simulation of the main phenomena involved on the structural response of the lining: (1) the steel fiber reinforced concrete (SFRC) post-cracking behavior, (2) the detailed behavior of the joints between segments and (3) the ground-structure interaction. The origin and the effects of all these phenomena and the modeling techniques employed to simulate them are carefully described and discussed. Finally, the results obtained are compared with the experimental evidences, showing the excellent accuracy achieved in terms of displacements, joints closures and crack patterns.

© 2011 Published by Elsevier Ltd.

1. Introduction

During last years, the evolution of the Tunnel Boring Machines (TBM) and the construction techniques associated to these drilling devices gave the opportunity to plan and construct tunnels under increasingly difficult scenarios. Nowadays, it is possible to construct tunnels under severe conditions and at any range of overburdens, with the possibility of achieving unsuspected drilling rates under high ground and water pressures. These unfavorable conditions imply higher structural requirements in order to resist the increments of ground pressures and the forces imposed by the advances of the TBM, conferring to the segmental tunnel lining a decisive role in the tunnel construction.

The optimization of segmental tunnel linings requires the utmost knowledge about the lining behavior and the structural forces that have to be resisted. Such like on the design practice of other structures, the prediction of linings behavior is commonly carried out by numerical models that simulate the conditions and phenomena imposed by the designers. Therefore, further to contrast the suitability of the adopted models it is also of paramount importance an appropriate selection and comprehension of the main phenomena involved in the structural response of the lining to achieve a better approach of the simulated situation. The behavior of segmental tunnel linings is affected by multiple phenomena that even individually present a complex behavior that significantly complicate the prediction of their structural response.

The *in situ* test performed on the experimental section of L9 tunnel of the subway of Barcelona (described in part 1 of this paper (Molins and Arnau, 2011)) represents, as far as known by the authors, a unique chance to determine the most important phenomena involved in segmental tunnel linings real behavior besides to allow the calibration and checking of the numerical models on the simulation of their structural response.

This paper deals with the numerical simulation of the *in situ* test and the comparison of the obtained results with the experimental evidences. In the first part, the main phenomena involved in the structural behavior of segmental tunnel linings are described and their modeling techniques are presented and discussed. These techniques are applied to the particular conditions of the experimental section of L9, defining both 2-D and 3D models to reproduce the test. The comparison of the experimental data with the numerical results in terms of general response, displacements, joints movements and crack patterns, allows the determination of the accuracy achieved with the proposed numerical models.

2. Tunnel behavior and associated phenomena

2.1. Phenomena common to all segmental tunnel linings

The models actually employed in the prediction of tunnel behavior are mostly created for design purposes. This fact allows the assumption of certain hypotheses that simplify the solution by providing safety results. On the other hand, the reproduction of the real response requires an adequate consideration of all parameters involved in that behavior. Therefore, it is necessary to

* Corresponding author. Tel.: +34 934017349; fax: +34 934054135.
E-mail addresses: oriol.arnau@upc.edu (O. Arnau), climent.molins@upc.edu (C. Molins).

clearly define them and develop numerical strategies for their accurate simulation.

Former approaches to predict the structural forces in tunnel linings were based on analytical solutions obtained from simplified models which considered the structure as a rigid pipe embedded on ground continuum model (Morgan, 1961; Muir Wood, 1975; Duddeck and Erdmann, 1985). The consideration of the ground-structure interaction was usually performed by means of the so-called bedded ring models, where the ground reaction is approached by means of discrete springs according to the Winkler's theory (e.g. Schulze and Duddeck, 1964). The analytical solution of these single models can neither take into account the complexities of the different phenomena involved in the structural behavior of segmental tunnel linings nor analyze complex situations suchlike a tunnel section crossing different ground layers. The use of the finite element method (FEM) allows the resolution of the bedded spring model for multiple load cases or support situations even including more advanced material properties or approximations to consider the effect of the joints between segments.

The adequate consideration of the joints behavior and its influence on the lining structural response have probably been the most discussed items in literatures regarding structural analysis of segmental tunnel linings. The first attempts to consider the influence of longitudinal joints were based on the increase of the lining flexibility. Muir Wood (1975) proposed a formulation to reduce the moment of inertia of a rigid pipe depending on the number of segments that composes the ring. Recent models consider the joints behavior by means of rotational springs located at joints places (JSCE, 2000; Blom, 2002; Ding et al., 2004), presenting the advantage of being easily implemented in bedded beam models. As it was defined by Blom (2002), the longitudinal joints present a complex non linear behavior due to their incapacity to transfer tensile stresses. For a certain axial stress level and an increasing bending moment, a loose of contact occurs at one side of the joint (joint gapping) generating a non linear behavior that is dependent on the axial stress. For the same joint, different axial stress levels provide different rotational behaviors, thus increasing the complexity of its appropriate consideration on the analysis models. In consequence, the main drawbacks of the rotational springs are the need of previous knowledge on the behavior of the implemented joint and the difficulty to take into account the influence of a certain axial stress level in the joint response.

More sophisticated approaches were used in shell elements models in order to achieve a better simulation of the real joint response. Vervuurt et al. (2002) modeled the joints between the shell elements segments by means of concrete beam elements which presented no tensile resistance whilst Van Empel and Kaalberg (2002) employed a combination of three springs to model their particular joint configuration. On approaches where the height of the structure is modeled by finite elements (plane stress models or 3D brick models) joints behavior is typically considered by means of interface elements placed at joints locations that do not allow the transmission of tensile stresses (Plizzari and Tiberti, 2006; Blom et al., 1999). This method represents the physical phenomenon occurring at the joint and, therefore, it is the most natural approximation to the real joint behavior.

Within the available bibliography it is assumed that a realistic simulation of segmental tunnel linings requires the consideration of the structural interaction between adjacent rings (coupled analysis) that is produced through the circumferential joints. The analyses performed by Klappers et al. (2006) show that the coupling of rings in segmental tunnel linings with staggered joints produce a stiffer structure respect of the aligned joints configuration. In consequence, higher bending moments are obtained with lower structure deformations. The coupling capacity of adjacent rings depends on multiple factors involving the joint configuration, the

axial stress remaining in the lining due to the TBM ram forces and also the ground stiffness due to its influence on the rings displacements and deformations. The lateral ring interaction is commonly modeled by means of coupling springs or interface elements located at contact points between adjacent rings. According to Blom (2002) those springs describe the combined behavior of the dowel and socket system and the lateral friction through packing materials.

Apart from the joints behavior, there is another parameter that significantly influences the structural response of tunnel linings: the ground-structure interaction. A ring of a segmental lining is a multiple hinged structure and, consequently, its equilibrium in front of loads depends on the surrounding ground response. The ground-structure interaction defines the boundary conditions of the structure and therefore its variation modifies the structural response of the lining. There are two main techniques for its modeling: (1) discrete springs assuming the Winkler hypothesis and (2) directly modeling the ground with finite elements. The full modeling of the ground with finite elements is mainly applied for analyses where surface settlements or accurate tunnel loads predictions are intended (e.g. Broere and Brinkgreve, 2002; Kasper and Meshke, 2004) while spring models are commonly used on the analyses focused on the structural behavior of the segmental concrete lining (e.g. Plizzari and Tiberti, 2006; Blom et al., 1999). Although the full modeling of surrounding ground should provide more accurate results (despite the fact that the interface conditions have also to be adequately selected), it requires heavy computational efforts when a detailed analysis with ground and structure non linear behaviors is intended. Additionally, the study of the lining structural response requires the evaluation of multiple structure, ground and load scenarios that suppose a tedious and difficult work to be created with the full ground modeling.

2.2. Particularities of the L9 experimental section

Besides the common phenomena associated to all segmental tunnel linings, the simulation of the *in situ* test requires the consideration of three particular phenomena occurring at the tested structure: (1) the use of steel fibers as unique reinforcement for concrete (only few small reinforcement bars were used to sustain the instrumentation of the test), (2) the use of bituminous packers in longitudinal joints (between segments of the same ring) which present a complex behavior and (3) the flat circumferential joints between rings.

2.2.1. Steel fiber reinforced concrete (SFRC)

The use of steel fibers in segmental tunnel linings has considerably increased during last years. Their main contribution is traditionally related to the avoidance of concrete spalling. Spalling is used to occur in segment joints due to deficient segment allocation, inadequate segment construction tolerances or joints geometries when the TBM jack forces are applied. Steel fibers act as small links between the detached concrete and the segment avoiding the repARATION of the superficial damage. But steel fibers are not only present at the edges or corners of the segments. Their presence inside the whole element may contribute to the structural resistance of the lining. Different works have been developed in order to quantify the contribution of steel fibers to the lining resistance (de Waal, 2000; Plizzari and Tiberti, 2006; Kasper et al., 2007). The *in situ* test aimed to perform a step forward and directly prove the suitability of using it as unique reinforcement. Moreover, the multiple data and the crack patterns obtained are used in the present paper to calibrate and contrast the precision offered by tunnel numerical models when the consideration of the structural contribution of such complicate material is intended. An accurate numerical simulation

will allow the study, comprehension and the design improvement of SFRC segmental tunnel linings.

2.2.2. Bituminous packer

The experimental section of L9 presents a singular joints configuration. Whilst the circumferential joints (between adjacent rings) present the usual plastic packers, the longitudinal joints (between segments of the same ring) present a 2 mm thick bituminous sheet instead of the more common concrete-to-concrete contact. During the characterization test of the packers carried out at UPC by Cavalaro (2009), a plastic behavior with significant remaining deformations was observed for the bituminous sheet. The *in situ* test comprises various load-unload cycles and consequently, the accumulation of plastic deformations causes different initial joint rotations at the start of each load phase. Therefore, it is necessary to accurately consider the packer behavior to obtain a satisfactory movements and displacements prediction.

An experimental campaign was carried out in order to determine the behavior of the L9 longitudinal joints packer. The test consists of 5 load-unload cycles with three different compression stresses (20, 40 and 60 N/mm²), repeating three times the maximum stress cycle. Fig. 1 shows the stress-strain relation obtained in the performed test.

As can be clearly observed in Fig. 1, the bituminous packer presents a non linear stress-strain diagram showing a soft behavior for low stresses and a hardening process close to 10 N/mm². A significant deformation remains in the packer after the unloading, presenting similar slopes for the unloading branches at different stress levels. The three consecutive cycles at 60 N/mm² denote a small additional remaining deformation despite the previous achievement of the stress level.

2.2.3. Flat circumferential joints

The circumferential joints do not present any dowel and socket system. In consequence, the transference of tangential forces is limited by the lateral friction between the concrete surface and the packers. Additionally, the experimental section was located inside a hard rock formation which severely limits the deformation of the loaded ring and consequently diminishing the coupling effect of the adjacent rings. Moreover, the results obtained in the *in situ* test showed that no significant stress redistributions occur from the loaded ring to the rest of the structure (Molins and Arnau, 2011). For this reason, it was decided to perform unique ring models to simulate the *in situ* test.

3. Modelization strategies

As previously mentioned, this work intends to evaluate the precision that can be achieved with the numerical models on the simulation of the structural behavior of segmental tunnel linings from

a practical engineering point of view. In this way, the most reasonable modeling philosophy goes through the simulation “one by one” of the main phenomena involved on the lining structural response and their subsequent integration in tunnel models. This section shows the numerical strategies followed to reproduce the material and physical behaviors that particularly affect the structural response of the test.

3.1. Steel fiber reinforced concrete (SFRC)

The experimental campaign carried out to characterize the SFRC of the segments is described in the part 1 of this paper (Molins and Arnau, 2011). The results of the 4 point beam tests (IBN, 1992) were used to determine the tensile behavior of the SFRC. This test provides the flexural post-cracking response of the SFRC by means of a load-deflection diagram, but the adequate material definition requires the tensile *versus* crack-opening response. The conversion factor that provides the crack-opening from the deflection was obtained through the geometrical analysis of the test configuration.

Steel fibers present a random distribution inside the concrete suck like aggregates and, therefore, can present multiple orientations. For this reason, the easiest and most common way to consider steel fibers contribution goes through the improvement of the post-cracking behavior of concrete.

In order to obtain the SFRC tensile behavior from the flexural response measured at 4 point beam tests, a simplified inverse analysis (Roelfstra and Wittmann, 1986) was applied. The SFRC sectional behavior described in the guidelines provided by Rilem TC 162-TDF (2003) was employed to determine the best-fitting post-cracking law according to a predefined function shape. Among the multiple possibilities of shapes that can be used to characterize SFRC post-cracking behavior (Antunes and Gettu, 2006), a sloped-constant diagram was selected (Fig. 2). The value of the load at first crack obtained in the NBN test was used to calculate the maximum flexural tensile stress of concrete ($f_r = 6.67$ N/mm²) and was converted to the maximum elastic tensile stress ($f_{cr} = 5.67$ N/mm²) by means of the formulation proposed in the Model Code (1990). Fig. 2 shows the results obtained on the inverse analysis to adjust the sloped-constant post-cracking diagram for the tested SFRC. With the aim of test and calibrate the numerical model of SFRC behavior, two different simulations of the 4-point beam test were carried out by means of plane stress and shell elements models. Both analyses were performed by means of the Multi-Directional Fixed Crack Model. This material model is based on the decomposition of the total strain into an elastic strain ϵ_e and a crack strain ϵ_{cr} , being necessary to define the stress-crack strain relation ($\sigma-\epsilon_{cr}$) for concrete tensile behavior. The conversion factor between crack-opening (ω) and crack strain (ϵ_{cr}) is the so-called crack bandwidth (h_{cr}) and corresponds to a numerical criterion based on the formulation of the finite elements (Bazant and Oh, 1983). In these analyses, it was assumed a crack bandwidth equal to the square root of the elements area ($h_{cr} = \sqrt{A_{el}}$). Additionally, for shell elements models, a geometrical equality between the side length of the element and the represented height was assumed.

As can be observed in Fig. 3, the results obtained from both type of models present a very good agreement to the experimental ones, thus validating the assumptions and modeling techniques used to define the SFRC post-cracking behavior.

3.2. Packer behavior

The modeling of the complex bituminous packer response (described at Section 2.2) was performed by means of a Von Mises plasticity model. The behavior presented in unloading and re-loading process is assumed to determine the elasticity modulus of the packer (670 N/mm²). A hardening diagram is employed to modify

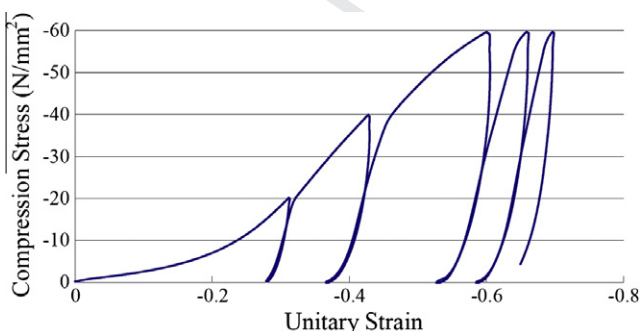


Fig. 1. Stress-strain relation for L9 bituminous packer under cyclic loading.

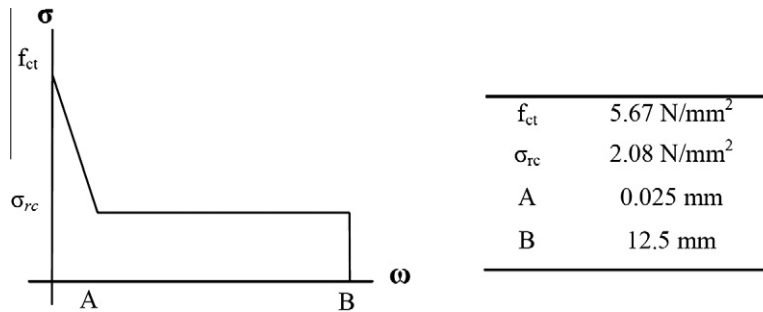


Fig. 2. Adopted sloped-constant diagram employed in the inverse analysis and its best fitting parameters to reproduce the experimental section SFRC behavior.

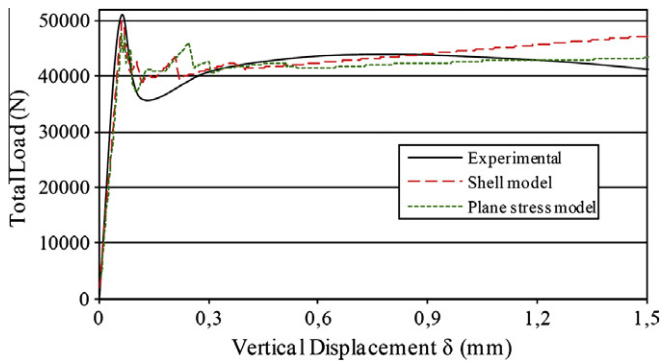


Fig. 3. Results obtained in the 4-point beam test simulations.

gapping is produced in tension. For shell elements model, a specific interface element with integration points along its height was used -CL24I, Diana 9 Manual (2005)-. The main limitation of this shell configuration in front of plane stress models is the incapacity to consider the local deformation of the concrete behind the packer (Fig. 6a). Despite this, no significant stress differences along the joint occur when comparing with results of the plane stress model, as can be seen in the example of Fig. 6b. The loose of contact on the upper part of the joint (around 200 mm in height) can also be observed in Fig. 6b, in which stress transmission zone is absent. This fact is particularly crucial because it allows the modeling of joints in an accurate way when using 3D shell elements models.

The combination of the packer behavior and the gapping phenomenon provides the nonlinear response of the joint that can be observed in Fig. 7. It shows the evolution of the rotational stiffness of L9 longitudinal joint for two different axial forces of 525 kN/m and 1050 kN/m, corresponding to a concrete compressive stresses of 1.5 N/mm² and 3 N/mm² respectively.

3.4. Ground-structure interaction

As previously discussed, the adequate consideration of the ground-structure interaction plays a decisive role on the structural simulation of segmental tunnel linings response. There exist two different elements that play a structural role beyond the segmental concrete lining: the hardened backfill grout and the surrounding ground (Fig. 8a). A bedded spring model was selected for the analysis of the *in situ* test, placing spring elements in radial (K_r) and tangential (K_t) directions (Fig. 8). The grout was simulated by means of interface elements placed between the structure and the ground spring elements. Fig. 8b shows the conceptual scheme for a plane stress configuration whilst Fig. 8c is related to the shell elements configuration.

the selected elasticity modulus in order to reproduce the initial load response of the bituminous packer. The simulation of the packer test was performed in order to contrast the suitability of the adopted model. The results are shown in Fig. 4.

The implemented model uses the same branch for the unloading and reloading processes presenting a small inaccuracy because it does not reproduce the additional plastic deformation occurred at every reloading, providing a slight underestimation of the total remaining deformation (Fig. 4) that should not affect the overall response of the ring.

3.3. Longitudinal joints

The simulation of the loose of contact in longitudinal joints was performed by means of unilateral interface elements located at one side of the plastic packer elements (Fig. 5). Nonlinear stiffness was assigned to them, defining a rigid behavior in compression whilst

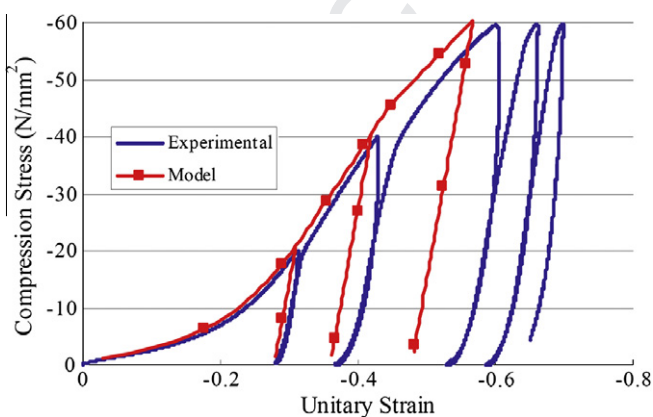


Fig. 4. Results of the simulation of the bituminous packer test.

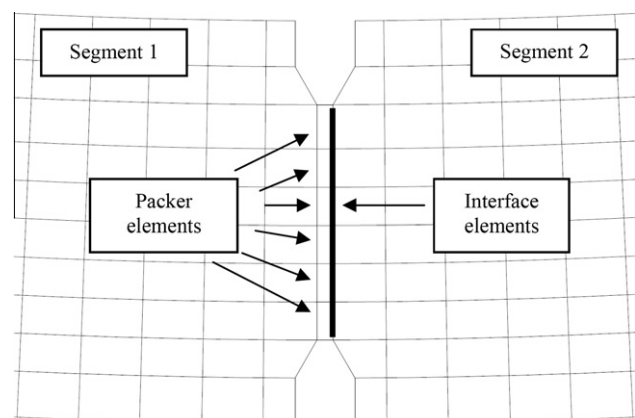


Fig. 5. Layout of joints configuration in plane stress finite elements model.

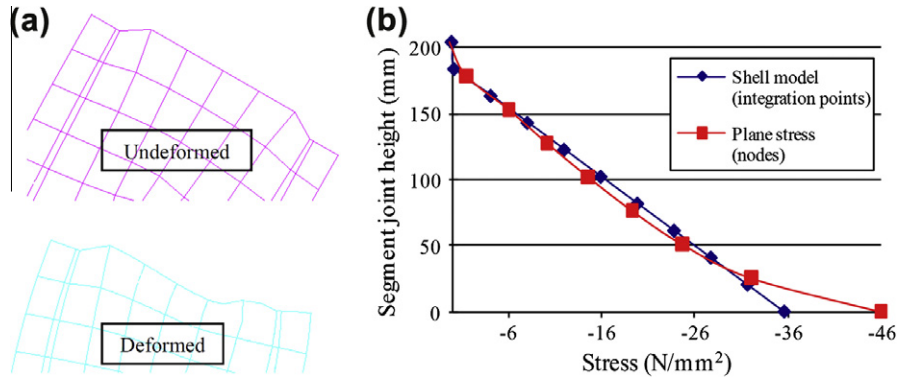


Fig. 6. Image of local concrete deformation at joints (a) and an example of its effect on the joint stress distribution (b).

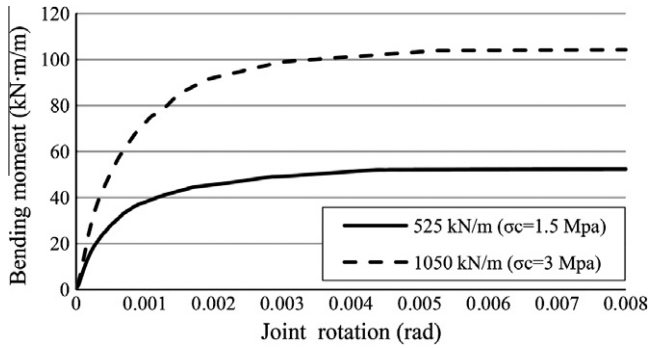


Fig. 7. Evolution of the rotational stiffness of L9 longitudinal joint for two different axial forces.

To consider the loose of contact between the lining and the grout a **Mohr-Coulomb** material model with tensile gap is applied to the interface elements. In consequence, when an interface element is subjected to a radial tension the gap arises, avoiding the transference of forces to the radial or tangential ground springs related to it. The compression stiffness of the interface elements is related to the gap size (175 mm in L9) and the grout elasticity modulus. For the latter, a value of 1000 MPa was estimated from the grout mix proportion, which is in accordance with the experimental results obtained at the district heating tunnel of Copenhagen described by Kasper et al. (2007).

The radial spring stiffness was assumed according to relation (1), corresponding to the analytical solution of a circular tunnel in elastic ground. Tangential stiffness (Eq. (2)), was assumed as 1/3 of the radial (Molins and Arnau, 2011). According to the geotechnical information, the parameters assumed to characterize the granodiorite rock formation surrounding the tunnel were an elastic deformation modulus of $E_s = 11,225 \text{ N/mm}^2$ and a Poisson ratio of $\nu = 0.24$.

$$K_r = \frac{E_s}{R \cdot (1 + \nu)} \quad (1)$$

$$K_t = \frac{K_r}{3} \quad (2)$$

4. Real scale test: numerical models and analyses

The previous modeling techniques of the different phenomena involved on the structural behavior of the L9 experimental section were applied on two different approaches: a 3D shell elements model and a 2D plane stress model. Both models only considered a unique ring regarding the quasi-individual response observed during the test (Molins and Arnau, 2011). Plane stress model should provide a more accurate sectional response due to the modeling of the segments height whereas the shell elements model can consider the effects of loads out of the middle plane. The latter is necessary in this case because the final position of the jacks was out of the middle plane of the ring. Table 1 shows the description and the amount of finite elements employed in each member of both models: 2D plane stress and 3D shell.

The reinforcement elements were used to simulate the small amount of reinforcement bars placed in the loaded ring to sustain the internal instruments. The steel plates located under the jacks were considered through the modification of the material properties of the affected elements.

Before the test simulation it was necessary to reproduce the previous state of the ring for three main reasons: (1) previous stress states play a decisive role on cracking formation and development, (2) the joints behavior depend on the real axial stress level and (3) the non linear behavior of bituminous packer, which presents high plastic deformation and a soft stiffness for low stress levels, determinates the ring displacements.

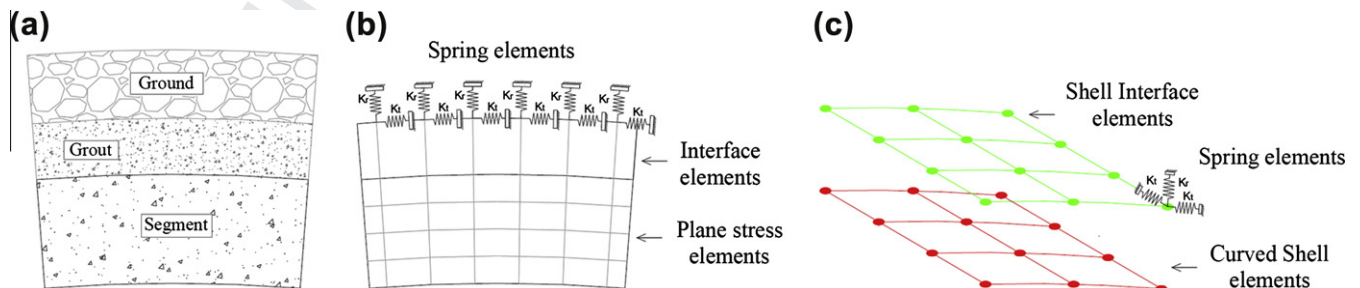


Fig. 8. Tunnel cross section scheme (a). Plane stress modeling (b) and shell elements modeling (c).

Table 1
Main characteristics of the *in situ* test performed models.

Shell model		Plane stress model		
Description	Quantity	Description	Quantity	
Nodes	3882		18,464	
Segments elements	Quadrilateral eight nodes curved shell elements (CQ40S)	525	Quadrilateral elements, eight nodes (CQ16 M)	5104
Plastic packer elements	Quadrilateral eight nodes curved shell elements (CQ40S)	40	Quadrilateral elements, eight nodes (CQ16 M)	32
Segment joints elements	Line interface shell elements, 3 + 3 nodes (CL24I)	40	Line interface elements, 3 + 3 nodes (CL12I)	32
Grout interface elements	Plane quadrilateral interface shell elements, 8 + 8 nodes (CQ48I)	525	Line interface elements, 3 + 3 nodes (CL12I)	735
Reinforcement elements	Reinforcement bar elements (Reinforcement)	844	Reinforcement bar elements (Reinforcement)	1458
Spring elements	Translation spring element, one node (SP1TR)	3746	Translation spring element, one node (SP1TR)	2956

Note: Diana 9 codification for each kind of element is specified in brackets.

Table 2
Load stages performed in the *in situ* test (Molins and Arnau, 2010).

Phase	Stage	Active jacks	Load/jack (kN)	Tunnel crown vertical deflection (mm)
0	1	Jack 1 + Jack 2 + Jack 3	100	-
1	2	Jack 1 + Jack 2	500	0.531
	3	Jack 1	500	0.022
	4	Jack 2	500	0.543
2	5	Jack 1 + Jack 2	1500	2.627
	6	Jack 1	1500	0.198
	7	Jack 2	1500	3.076

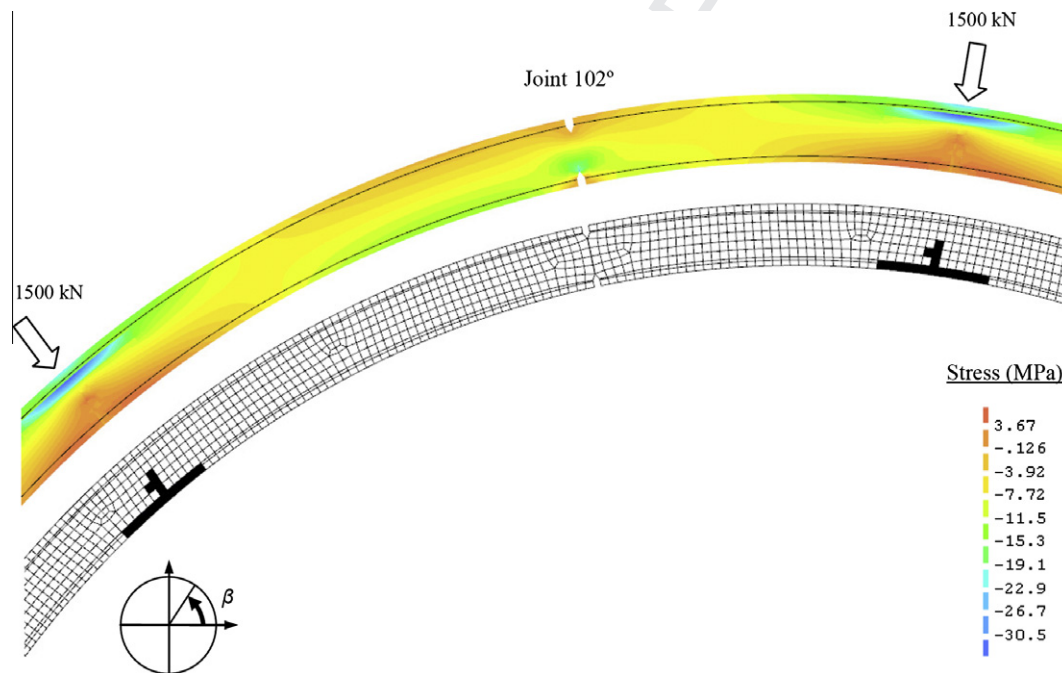


Fig. 9. Circumferential stress during stage 5 (MPa) and cracked elements (in black).

The experimental section was located inside a hard granodiorite rock formation that was resistant enough to generate a self-stable excavation and, hence the ground almost did not generate external pressures over the lining, as proved the measurements of the instruments. Consequently, it was supposed that the initial load over the lining was caused by the hydraulic pressure of the ground water. This pressure was obtained from the load cells placed at the extrados of the experimental ring and was applied to the numerical models to perform the initial situation analysis. In order to correctly simulate the tunnel construction process, the ground-structure interaction was remained inactive in this initial phase. Water pressure acts prior to the backfill grout hardening which fix the lining to the ground and marks the start of the transmission

of forces between the lining and the ground. After the analysis of the initial state, the same load procedure followed during the *in situ* test was reproduced. The load stages described in Table 2 were sequentially applied, considering that every stage is defined by a loading and unloading cycle (Molins and Arnau, 2011). The jack forces were applied by means of distributed loads according to the real placement and surface of the jacks.

5. Analysis of the results

The results obtained in the numerical simulation of the test, which are presented along this section, are compared with the experimental measurements to analyze their validity and

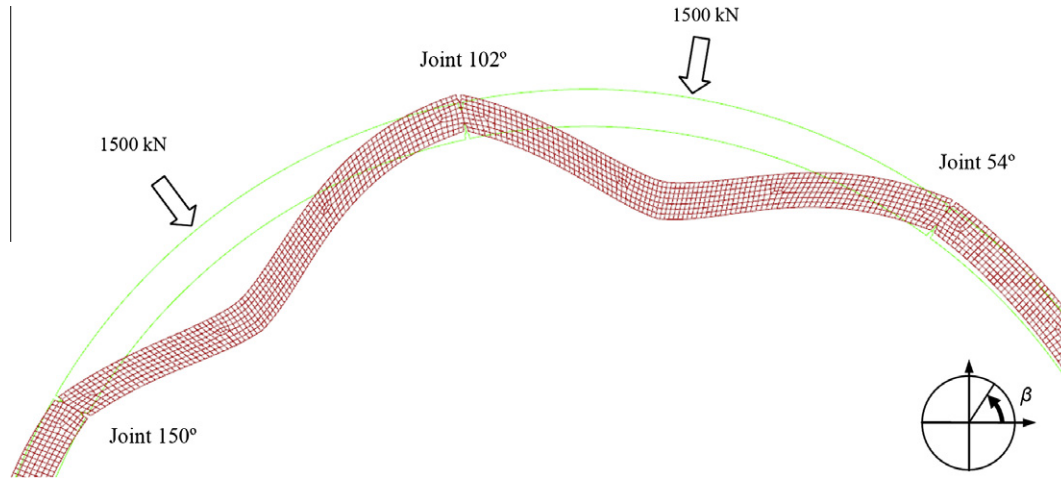


Fig. 10. Tunnel crown deformed shape during stage 5 (amplification factor = 300).

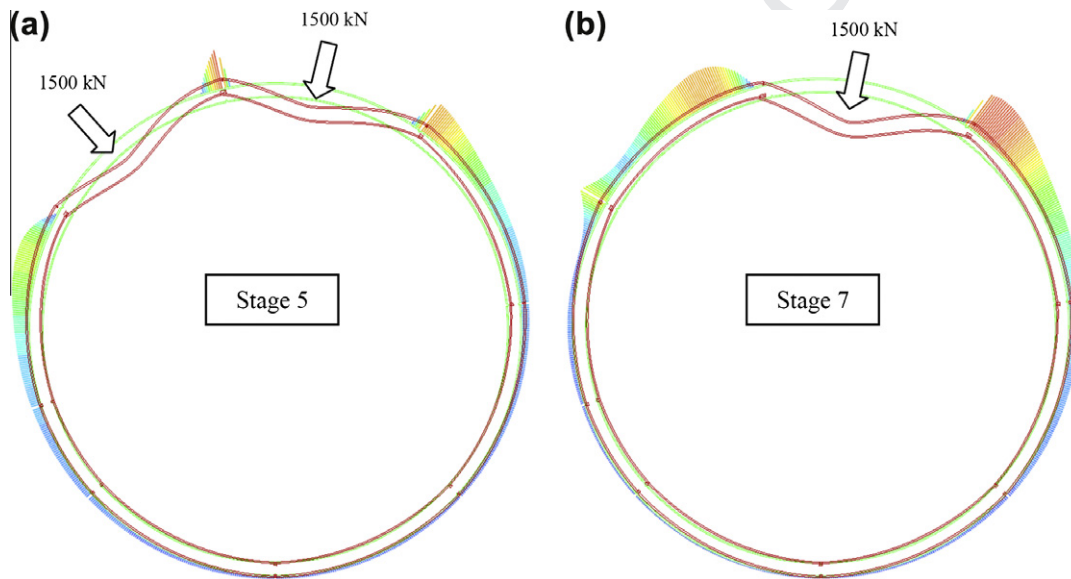


Fig. 11. Radial ground response in stages 5 (a) and 7 (b) and associated deformed shapes (in red). (For interpretation of the references to colour in this figure legend, the reader is referred to the web version of this article.)

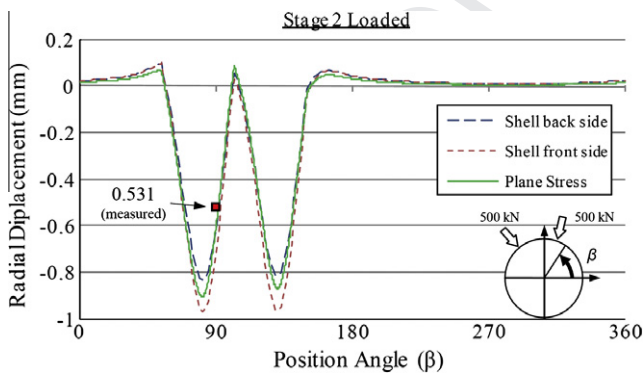


Fig. 12. Comparison of results of radial displacement at stage 2.

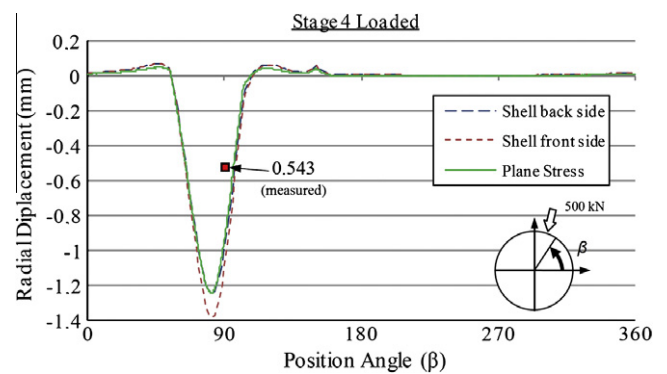


Fig. 13. Comparison of results of radial displacement at stage 4.

5.1. General behavior

453

451 precision. The comparison is carried out in terms of general behavior, displacements, joints movements and crack patterns.

454 Fig. 9 shows the circumferential stresses predicted by the plane stress model on the tunnel crown zone and the finite elements

454

455

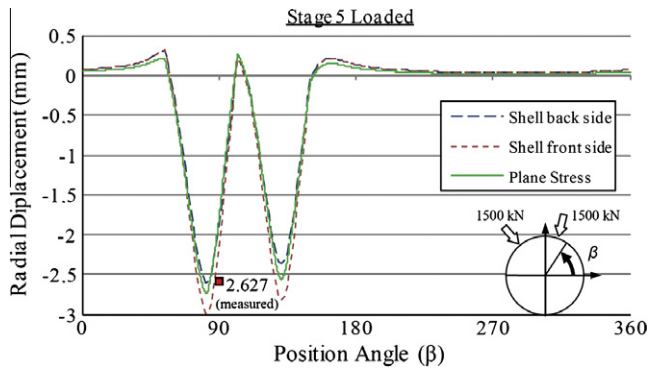


Fig. 14. Comparison of results of radial displacement at stage 5.

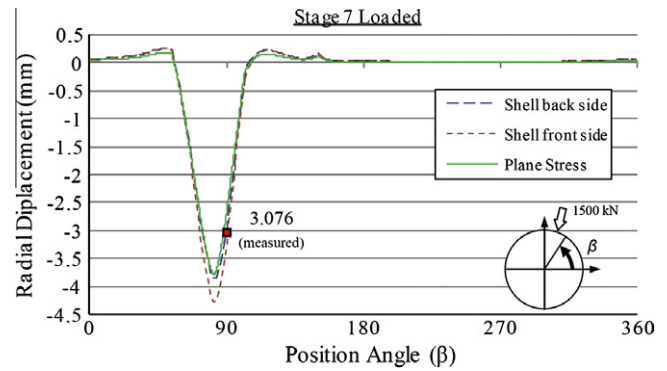


Fig. 15. Comparison of results of radial displacement at stage 7.

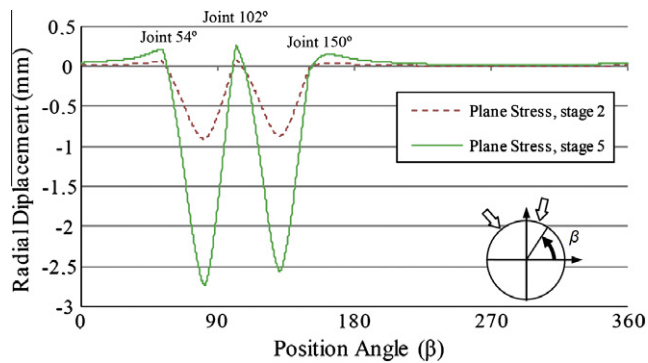


Fig. 16. Radial displacement obtained in plane stress model at stages 2 and 5.

One of the most important conclusions from the *in situ* test (Molins and Arnau, 2011) was that, for hard ground conditions, the ring response under concentrated loads is related to an arch behavior that directly discharge the load to the ground. This fact produces a resisting mechanism which is concentrated nearby the zone where the loads are applied. Fig. 11a and b shows the numerically obtained radial ground response for stages 5 and 7 and the associated deformed shape of the ring respectively.

In both cases, the radial response clearly denotes the zone where the arch is pressuring the ground and how the rest of the ring does not present any significant interaction. Consequently, the structural response of the ring under concentrated loads in hard ground conditions is limited to the behavior of the zone close to the loads appliance points.

5.2. Displacements

The radial displacement obtained by both models for stages 2, 4, 5 and 7 and the experimental measurements are presented in Figs. 12–15. For the shell model, the displacements of the two segment edges are presented. Jack 1 was located far from the tunnel crown and, in consequence, its isolated action (stages 3 and 6) did not generate significant movements on the instruments placement (Table 2). For this reason, the numerical results obtained for these stages are not presented.

The vertical displacement of the tunnel crown obtained in the numerical models (radial displacement at $\beta = 90^\circ$) shows a very good agreement with the experimental results (Table 2, and square point in figures). Plane stress and shell models present very similar results for all loading stages. The vertical displacement obtained for stages 2 and 7 presents an excellent accuracy whilst the analysis of stage 5 shows a slight underestimation in front of the

affected by cracking at stage 5 (Table 2), corresponding to a load of 1500 kN per jack. Joint non linear behavior can be clearly appraised through the absence of tensile stresses at the extrados side of the joint at 102° and the concentration of compressions at the intrados side. Equally as observed during the test, cracking is only present at the intrados of the locations of the jacks. At these points, compression stresses are observed at the extrados, including a concentration at the steel plate.

The numerical simulations reproduce the same mechanism governing the displacements of the loaded ring observed experimentally. As can be seen in Fig. 10 where the plane stress model deformed shape for stage 5 is shown, ring movements are mainly caused by concentrated rotations in longitudinal joints and in the cracked sections under the jacks.

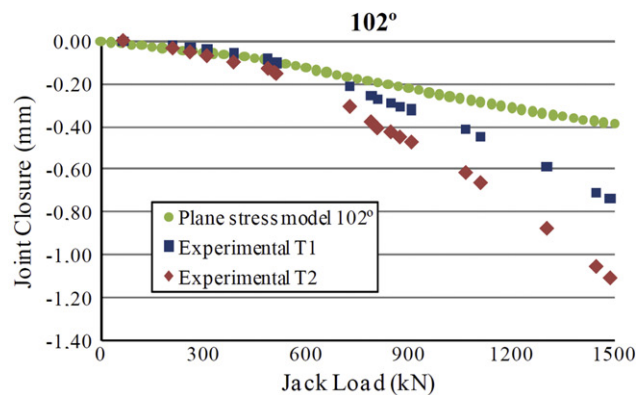
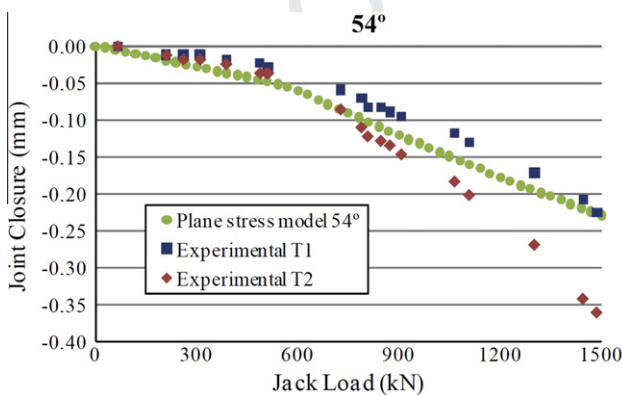


Fig. 17. Evolution of joints closure (intrados side) at 54° and 102° during stage 5.

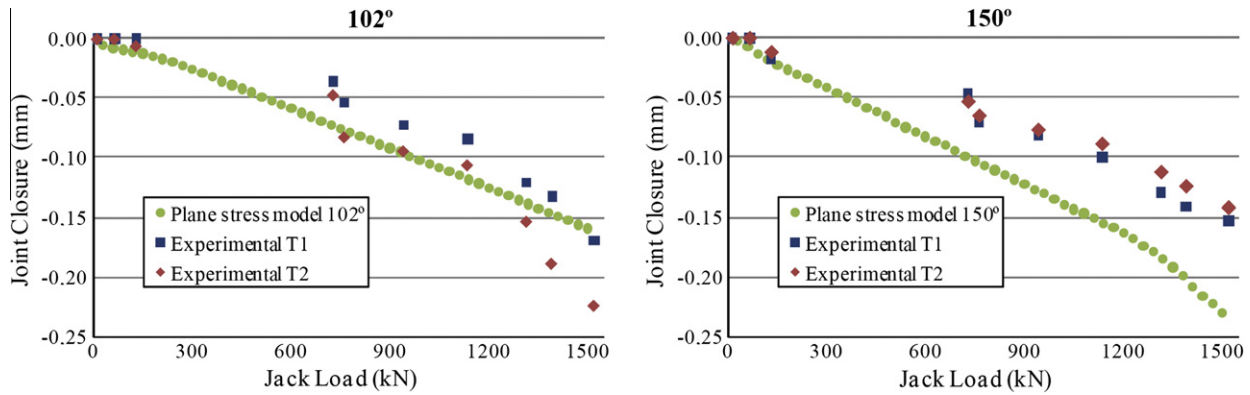


Fig. 18. Evolution of joints closure (intrados side) at 102° and 150° during stage 6.

experimental data. A small overestimation of the measured movement is obtained for stage 4. In fact, the measured result is not in concordance with the tendency of each load configuration because the isolated action of jack 2 (stages 4 and 7) should provide higher crown displacements than the simultaneous action of jacks 1 and 2 (stages 2 and 5). It is also important to notice that displacements are mainly concentrated under the jacks and, in consequence, present a high variation in a short distance. In consequence, some small variations in the test instruments positions can provide differences like the obtained between the experimental and the numerical results.

The effects of the final eccentricity of the jacks caused by its deficient allocation can be observed in shell elements model results. The displacements obtained in the ring front side are always higher than the ones obtained in the back side, thus showing the non-uniform deflection of the ring.

Fig. 16 shows the comparison of the radial displacements obtained for the configurations where jacks 1 and 2 acts simultaneously (stages 2 and 5). The load increase does not entail a widest descent zone, maintaining it between the joints. In consequence, the increase of the radial displacement is originated by higher rotations in joints and in the cracked sections under the jacks. In fact, both analytical and experimental results coincide that no cracking is produced during stage 2.

5.3. Joints movements

The comparison of the evolution of joints closures obtained experimentally and analytically during the stages 5 and 6 of the test are presented in Figs. 17 and 18. Experimental results in joints were measured by displacement transducers (T1, tunnel side, and T2, excavation side) placed at the intrados of the loaded ring between segments A1-A2 (54°), A2-A3 (102°) and A3-B (150°).

As can be clearly observed in both graphs of Fig. 17, the evolution of joints closure perform a sudden variation for a jack load close to 600 kN which is caused by the start of joint gaping due to the loose of contact at the extrados side. The evolution of closure at 54° joint presents a very good fitting to the experimental results, whereas the results at joint 102° present some differences for high load values. On the other hand, the evolution of 102° joint closure during stage 6 perfectly fits with the numerical prediction (Fig. 18) whilst the 150° joint is the one that present some differences. This fact means that the small inaccuracy of the numerical model should be caused by the imprecision of some input parameters more than the strategies used to model the different phenomena involved on the structural response of the ring. The agreement obtained in the radial displacements shows that these differences might be caused by small variations on the distribution of the concentrated rotations between the joints and the cracked sections. If the radial ground

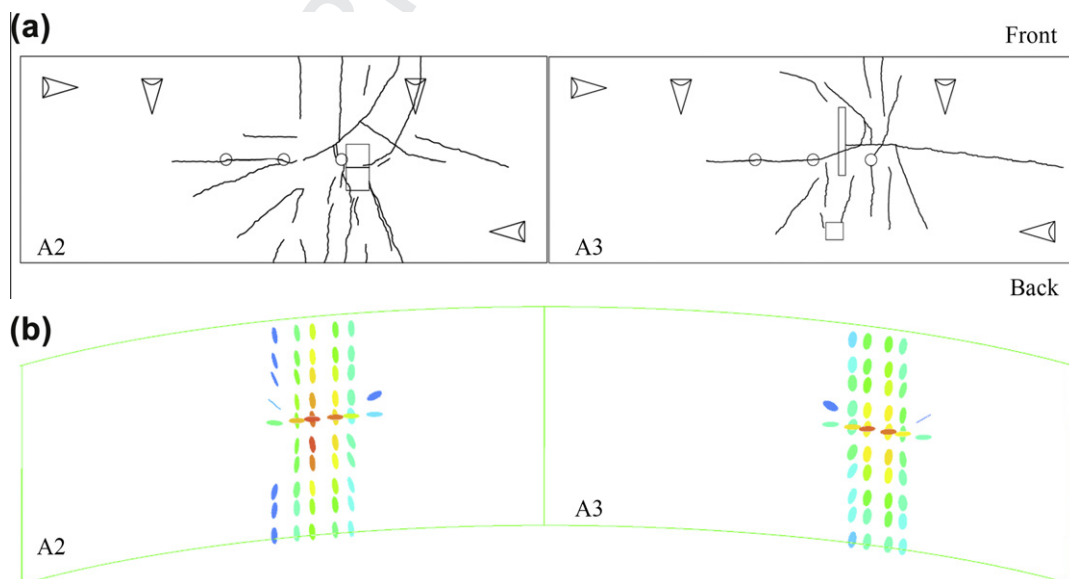


Fig. 19. Crack patterns obtained at the *in situ* test (a) and by the shell numerical model (b).

stiffness is slightly overestimated the flexibility of the arch mechanism is reduced, diminishing the rotations experimented at joints. Consequently, to obtain the same ring deformation, higher rotations have to be concentrated on the cracked sections.

5.4. Crack patterns

The experimental crack pattern observed at stage 5 and the one obtained using the shell model are presented in Fig. 19. The numerical model fits very well the general tendency of ring cracking. As was previously described, cracks appear exclusively under the jacks (this fact was also confirmed by the plane stress model, Fig. 9), but the 3D features of the shell model provide improved information about the cracking prediction skills of the presented numerical models. The main cracks that appear in the longitudinal tunnel direction have the expectable orientation due to the bending moments produced in the ring by the load. Furthermore, the shell model is capable to reproduce the circumferential cracks (horizontal in Fig. 19) and, in minor extent, the cracks that appear on radial orientation from the jacks positions. Both cracks are caused by local bending stresses derived from the spreading of the jacks loads across the segment. Finally, it is worth noting that the analytical results fit the widest damage zone (with more longitudinal cracks) that was recorded in the experiment for the segment A2.

6. Conclusions

The simulation of the complex *in situ* test carried out in its definitive position inside a real tunnel is presented in this paper. The test presents the advantage of providing the real structural response of a certain tunnel section by taking into account all the parameters that affect it, from the most important to the less relevant. The knowledge about the real segmental tunnel lining behavior gives the insights of which are the main phenomena affecting its response and, consequently, the most affecting on numerical simulations. Within this process there are a lot of secondary parameters, mainly caused by the tunnel construction process (backfill grout influence, irregular segments connections, etc.), that can affect the precision of the analytical results but should not be determinant on the behavior of the segmental tunnel lining. Additionally, the exactitude of some parameters assumed in the model is questionable (for example, the ground elastic modulus and its homogeneous distribution around the whole tunnel) and this may also affect the precision of the model. Despite these facts, the analysis of the results obtained in the simulation of the *in situ* test performed by the aforementioned numerical models and its comparison with the experimental evidences showed that:

- The lining behavior obtained by the numerical model perfectly fits to the real one deduced from the test measurements. The local arch behavior and the rings displacements caused by joints and cracked sections rotations were clearly appraised.
- The accuracy shown in the displacements predictions through all the loading process confirms the validity of the adopted modeling philosophy, hypothesis and techniques.
- The similarities obtained between the real and the numerical crack patterns corroborate the suitability of the adopted model on taking into account the steel fibers contribution to the structural response of the lining.
- The obtaining of the real structural response of segmental tunnel linings requires the realistic simulation of: (1) the unilateral behavior of joints, including the packing material response if it exists, (2) the ground-structure interaction, considering the tangential effects and the loose of contact, and (3) the cracking of concrete for high load scenarios such as applied to L9 tunnel during the *in situ* test.

For these reasons, it can be concluded that the structural behavior of SFRC segmental tunnel linings can be accurately simulated by adopting the appropriate hypothesis and modeling techniques.

Acknowledgements

This research was possible thanks to the support provided by GISA, the public company of the Generalitat de Catalunya responsible of the design and construction of L9 and by FCC Construcción, S.A. The first author also wants to thank the support of the University and Research Commissioner of the DIUE of the Generalitat de Catalunya and also the European Social Fund (ESF).

References

- Antunes, J.L., Gettu, R., 2006. Determining the tensile stress–crack opening curve of concrete by inverse analysis. *Journal of Engineering Mechanics* 132 (2), 141–148.
- Bazant, Z.P., Oh, B.H., 1983. Crack band theory for fracture of concrete. *Materiaux et constructions* 16 (93), 155–177.
- Blom, C.B.M., van der Horst, E.J., Jovanovic, P.S., 1999. Three-dimensional structural analyses of the shield-driven “Green Heart” tunnel of the high-speed line South. *Tunnelling and Underground Space Technology* 1 (2), 217–224.
- Blom, C.B.M., 2002. Design philosophy of concrete linings for tunnels in soft soils. Ph.D Thesis. Technische Universiteit Delft.
- Broere, W., Brinkgreve, R.B.J., 2002. Phased simulation of a tunnel boring process in soft soil. *Numerical Methods in Geotechnical Engineering*. Presses de l'ENPC/LCPC, pp. 529–536.
- Cavalaro, S.H.P., 2009. Aspectos tecnológicos de túneles construidos con tuneladora y dovelas prefabricadas de hormigón. Ph.D Thesis. Universitat Politècnica de Catalunya (in Spanish).
- CEB-FIP, 1990. Model Code for concrete structures (MC-90).
- Ding, W.Q., Yue, Q.Z., Tham, G.L., Zhu, H.H., Lee, C.F., Hashimoto, T., 2004. Analysis of shield tunnel. *International Journal for Numerical and Analytical Methods in Geomechanics* (58), 57–91.
- Duddeck, H., Erdmann, J., 1985. On structural design models for tunnels in soft soil. *Underground Space* 9, 246–259.
- Institut Belge de Normalisation (IBN), 1992. Essais des Bétons Renforcés de Fibres – Essai de flexion sur éprouvettes prismatiques, NBN B 15-238 (in French).
- JSCE (Japan Society of Civil Engineers), 2000. Japanese Standard for Shield Tunnelling. The third edition.
- Kasper, T., Meshke, G., 2004. A 3D finite element simulation model for TBM tunnelling in soft ground. *International Journal for Numerical and Analytical Methods in Geomechanics* 1 (28), 1441–1460.
- Kasper, T., Edvardsen, C., Wittneben, G., Neumann, D., 2007. Lining design for the district heating tunnel in Copenhagen with steel fibre reinforced concrete segments. *Tunnelling and Underground Space Technology* 23, 574–587.
- Klappers, C., Grübl, F., Ostermeier, B., 2006. Structural analyses of segmental lining – coupled beam and spring analyses versus 3D-FEM calculations with shell elements. In: *Proceedings of the ITA-AITES 2006 World Tunnel Congress, Safety in the Underground Space*. 6 pp.
- Molins, C., Arnau, O., submitted for publication. Experimental and analytical study of the structural response of segmental tunnel linings based on an *in situ* loading test. Part 1: Test Configuration and Execution. *Tunnelling and Underground Space Technology*.
- Morgan, H.D., 1961. A contribution to the analysis of stress in a circular tunnel. *Géotechnique* 11 (1), 37–46.
- Muir Wood, A.M., 1975. The circular tunnel in elastic ground. *Géotechnique* 25 (1), 115–127.
- Plizzari, G.A., Tiberti, G., 2006. Steel fibers as reinforcement for precast tunnel segments. In: *Proceedings of the ITA-AITES 2006 World Tunnel Congress and 32nd ITA General Assembly*. 6 pp.
- Rilem TC 162-TDF, 2003. Test and design methods for steel fibre reinforced concrete. σ – ε Design method. Final recommendation. *Materials and Structures* 36, 560–567.
- Roelfstra, P.E., Wittmann, F.H., 1986. Numerical method to link strain softening with failure of concrete. In: Wittmann, F.H. (Ed.), *Fracture Toughness and Fracture Energy of Concrete*. Elsevier Science, pp. 163–175.
- Schulze, H., Duddeck, H., 1964. Statische Berechnung Schieldvorgetriebener Tunnel (Structural analysis of tunnels excavated with shield support). *Beton und Monierbau AG 1889–1964*, 87–114.
- TNO, 2005. Diana user's manual. Release 9. <<http://www.tnodiana.com>>.
- Van Empel, W.H.N.C., Kaalberg, F.J., 2002. Advanced modeling of innovative bored tunnel design Amsterdam North-Southline. In: *Proceedings of the DIANA World Conference*. Tokyo, pp. 439–448.
- Vervuurt, A.H.J.M., Van del Veen, C., Gijsbers, F.B.J., Den Uijl, F.B.I., 2002. Numerical simulations of tests on a segmented tunnel lining. In: *Proceedings of the DIANA World Conference*. Tokyo, pp. 429–437.
- De Waal, R.G.A., 2000. Steel fibre reinforced tunnel segments for the application in shield driven tunnel linings. Ph.D Thesis. Technische Universiteit Delft.